Spectroscopic imaging by two-dimensional electrooptic sampling in the terahertz region

H. KITAHARA[a,*], M. TANI[b], M. HANGYO[b]
[a]*Research Center for Development of Far-Infrared Region, University of Fukui, 3-9-1 Bunkyo Fukui, Fukui 910-8507, Japan*
[b]*Institute of Laser Engineering, Osaka University, 2-6 Yamadaoka, Suita, Osaka 565-0871, Japan*

A terahertz (THz) time-domain imaging system is developed based on two-dimensional electrooptic sampling with a high-speed complementary metal-oxide semiconductor camera. Spectroscopic images are observed under nondestructive and noncontact conditions to demonstrate transmissive imaging of an L-cystine chip embedded in a polyethylene pellet. Time waveforms that have a time period of 68.1 ps are acquired for 16384 pixels within six minutes during the observation. The L-cystine chip, which has a fingerprint spectrum in the THz region, is depicted clearly in the spectroscopic image at the fingerprint frequency by reassembling the image from the spectrum obtained by Fourier transform of the acquired time waveforms.

(Received September 3, 2018; accepted November 29, 2018)

Keywords: THz, Time-domain spectroscopy, Spectroscopic imaging, Two-dimensional imaging

1. Introduction

Imaging by terahertz (THz) pulse waves has been actively studied as for nondestructive and noncontact applications because of the absence of damage to materials caused by THz waves. For example, inspection of the medication quantity included in a multi-layered pill is requested to control the quality at the factory that is producing the pill in large quantities [1]. When the medication included in a layer inside the pill has a characteristic fingerprint spectrum in the THz region and the outside layer is transmissive for THz waves, the distribution image of the specific constituent inside the pill can be depicted by observation of the THz wave. THz imaging systems are suitable for pharmaceutical and medical applications because they have the ability to perform nondestructive inspection of the measured object without ionization of the component materials [2-9].

The most pressing problem in the application of THz imaging is the comparatively long measuring period of the image scan, when the image data is acquired at high speed. Because imaging systems have been fabricated primarily based on THz time-domain spectroscopy (THz-TDS) until now, a great amount of time is spent on the image scan if the time scan is performed at each pixel that comprises an image. Performance improvement has been attempted by improving the radiation intensity using a high-power emitter, as well as increasing the image acquisition speed using a high-speed optical delay line or asynchronous optical detection [10-26].

A detection method where two-dimensional (2D) information is acquired at one time by combining electrooptic (EO) sampling and a digital camera has been reported as an alternative method for improving the scan speed [27-33]. There are two data acquisition methods in 2D-EO. One acquires 2D real space information, and the other acquires information concerning one-dimensional real space and the time-domain. Each method acquires spectrum information for individual image pixels by scanning the remaining dimension or domain. The image acquisition becomes considerably faster using the 2D-EO sampling that acquires the image information at one time compared with the imaging system that consists of THz-TDS involving zero-dimensional detectors, such as a photoconductive antenna. The most recent complementary metal-oxide semiconductor (CMOS) camera currently available can easily operate at the repetition rate of a fs-laser system. When an observation with a single laser shot is performed using a high-intensity THz emitter at low repetition rate and a high-speed CMOS camera under the ideal acquisition period of 10 ms, we can expect to acquire a spectroscopic image within one second. However, an integration of one thousand shots is often required because of the degradation of the signal-to-noise ratio (SNR) caused by the intensity fluctuation of the laser beam from pulse to pulse. The measurement time is still high-speed, while the data acquisition requires from three to six minutes.

The spectroscopic imaging made possible by high-speed 2D-EO sampling is one technique for mapping the material in an object [34]. Mapping using the intensity cannot distinguish the distribution of component materials

with similar refractive indexes in composites. Conversely, the spectroscopic image acquired at the fingerprint frequency can distinguish the distribution of each material in the composite. The spectroscopic imaging of the object contained the metamaterial flakes with the well-defined and sharp absorbance line is one of the examples of such case. [35] Accordingly, this technical problem should be clarified to improve the performance of THz spectroscopic imaging, and an improvement strategy should be planned.

In this paper, we construct a THz time-domain imaging system based on THz-TDS using 2D-EO sampling, a high-speed CMOS camera, and a regenerative amplified titanium-sapphire laser source. Spectroscopic imaging is conducted for an L-cystine chip embedded in a polyethylene pellet and demonstrated using the THz spectroscopic information of the fingerprint frequency of 725 GHz.

2. Operating principle of the imaging system

The THz imaging system is constructed based on two-dimensional electrooptic sampling and THz-TDS. The EO crystal is irradiated by a large-diameter THz beam to acquire a THz image of the sample. The THz emitter needs to be a high-intensity device to increase the electric field amplitude at the surface of the EO crystal. A large-aperture antenna or a nonlinear optical crystal is generally used for the emitter. A femtosecond laser that has a high peak pulse power is used as an excitation laser source for these emitters. THz images are acquired by the direct-subtraction method to reduce the large noise included in low-frequency components compared with the repetition rate of the laser [36]. The THz electric field radiated from the emitter is modulated by the intermittent pump pulses, as shown in Fig. 1. The generated THz wave is transmitted to the detector with a pass through the THz optics. The polarization of the probe beam is modulated at the EO crystal by the THz electric field. The 2D image of the probe beam is acquired by the high-speed camera while synchronizing with the THz pulse wave after analysis by the polarizer. Because these images are superimposed by the background noise with identical phase, the foreground $\mathbf{Img}_{on}$ and background $\mathbf{Img}_{off}$ are processed to obtain the image of the electric field $\mathbf{Img}_{sig}$ that can effectively eliminate the noise using the following equation:

$$\mathbf{Img}_{sig}(k) = \mathbf{Img}_{on}(2k) - \mathbf{Img}_{off}(2k\text{-}1), \qquad (1)$$

where **Img** is a matrix composed of the pixel data of the camera. The remaining noise component is eliminated by performing time integration of the $\mathbf{Img}_{sig}$. The raw structural data of the sample is acquired by integrating the $\mathbf{Img}_{sig}$ at each time delay while changing the detection timing.

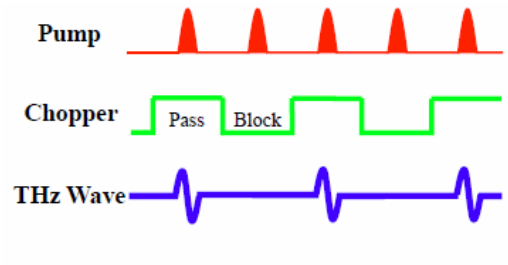

Fig. 1. Emitted THz wave and chopper state with laser emission

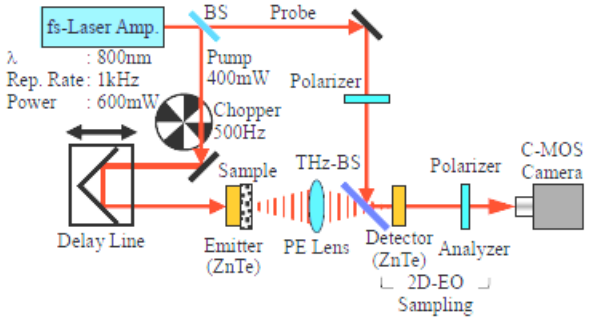

Fig. 2. Block diagram of THz 2D-EO imaging system. Thick short lines at the corner of the laser beam represent mirrors and beam splitters

3. Experimental setup

The block diagram of the THz imaging system is shown in Fig. 2. The laser source is a fs-laser (Hurricane, Spectra Physics Inc.) with a regenerative amplifier and 1-kHz repetition rate. The laser beam with a 5-mm diameter is divided by the beam splitter (BS) to prepare a pump and a probe beam. The pump beam of 200 mW is irradiated to the emitter of 1.5 mm thickness made of zinc telluride (ZnTe) crystal after being transmitted through an optical chopper and an optical delay line. The optical chopper is synchronized with the half frequency of the laser repetition rate. A nearly collimated THz beam 5 mm in diameter is radiated from the emitter. The sample is placed just behind the emitter. The THz wave transmitted through the sample forms an image on to the ZnTe crystal that is 2.5 mm thick using a polyethylene (PE) lens with a focal length of 60 mm. The diameter of the probe beam that was adjusted to 60 mW by a variable neutral density filter is magnified to 20 mm by a beam expander. The probe beam is collimated to the THz wave by a high-resistivity silicone BS after trimming the beam diameter to 15 mm using an iris. The 2D-EO detector is composed of a ZnTe crystal and a polarizer aligned to nearly-zero optical bias. A high-speed CMOS camera that has 128x128 pixels acquires a 2D-EO image. Because the composition of the imaging system acquires a 2D real-space image, the time waveform is measured by scanning the optical delay line.

The observable area was 5 mm in height and 4 mm

wide. The amount of acquired time waveform was 16384 data sets.

The acquisition of such a large amount of data in a short time is a very hard task for a raster-scan type imaging system. However, the 2D-EO THz imaging system was able to make a two-dimensional time waveform scan within 6 min for 256 sampling points. When the spatial resolution is defined as the full width at half maximum (FWHM), the resolution in the plane perpendicular to the propagation direction of the THz wave was 0.6 mm, which is almost equal to the peak wave length of the radiated spectrum from the emitter. This spatial resolution is almost as good as that of the ordinary THz-TDS imaging system. The SNR of the amplitude at the center of the image was about 100, which is lower than that obtained with a typical THz-TDS imaging system. The low SNR is caused by the laser pulse fluctuation, with a range of 5%, and low intensity of the THz wave at the EO crystal. Simply, it is possible to improve the SNR using a high-repetition rate amplified laser and a tilted-pulse-front emitter. However, the most noticeable problem for the 2D-EO imaging is the intensity fluctuation within the cross-section of the laser beam and the nonuniformity of sensitivity in the detecting area caused by the residual birefringence of the EO crystal. These problems degrade the image quality markedly. In particular, a light source is required to improve the beam quality because the fluctuation within the cross-section of the laser beam, which varies with every pulse, is difficult to correct using an outside system.

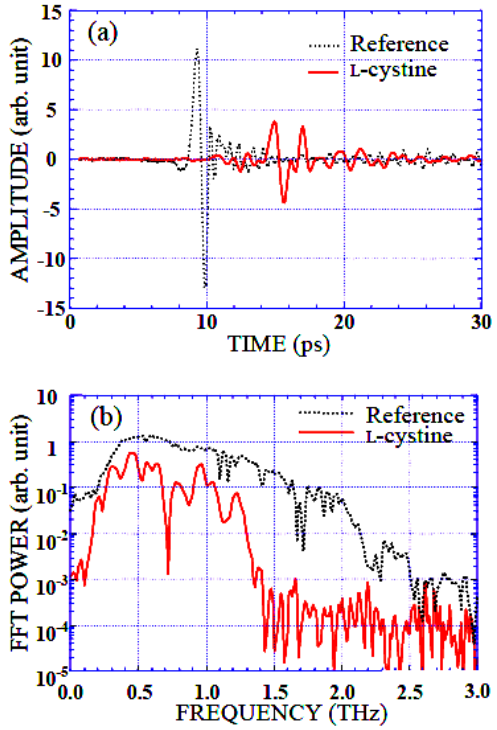

Fig. 3. Observation result of (a) time waveform and (b) power spectrum

4. Acquisition of THz spectroscopic image

A transmission spectrum was measured to examine the fingerprint frequency of L-cystine before the observation of the spectroscopic imaging. Figure 3(a) and 3(b) show the time waveform and transmission spectrum, respectively. The reference is shown by a dotted line, and L-cystine is shown with a solid line. An L-cystine pellet with a thickness of 1.5 mm was measured in atmosphere at ordinary temperature and pressure. The image data consisting of 500 frames were integrated at each measuring point in the experiment. The 512 measuring points were measured with a time-delay interval of 133.3 fs. The graphs of Fig. 3 depict the pixel at the center region of the acquired image. The transmission spectrum, which has a transmissive region up to 1.4 THz, contains a fingerprint spectrum of the absorption at 725 GHz. The spectroscopic imaging is performed at this frequency.

A sample for measurement was fabricated to conduct the spectroscopic imaging of L-cystine embedded in a pellet. Fig. 4 shows a schematic illustration of the sample, which consists of an embedded L-cystine chip in the form of an equilateral triangle with sides of 3 mm and thickness of 0.4 mm in a polyethylene pellet with a diameter of 13 mm and thickness of 0.8 mm. The center region of the sample that included an L-cystine chip was measured in atmosphere at ordinary temperature and pressure. The 256 measuring points were measured with a time-delay interval of 66.7 fs. The resolution of the spectrum was evaluated at 58.6 GHz from the interval of the time-delay. The spectrum information was obtained by Fourier transform of the time-waveform of each pixel. The transmission spectrum was obtained from the observed data of the sample and the reference at each frequency for each pixel. Then, the image was reassembled at each frequency. Spectroscopic images of the fingerprint frequency of 725 GHz and of the transmissive frequency of 505 GHz are shown in Fig. 5(a) and 5(b), respectively. The image was acquired for an area of 4 × 4 mm^2, and white color shows the low-transmission region. Figure 5(a) shows high transmission uniformly, whereas Fig. 5(b) clearly shows the triangular shape of L-cystine.

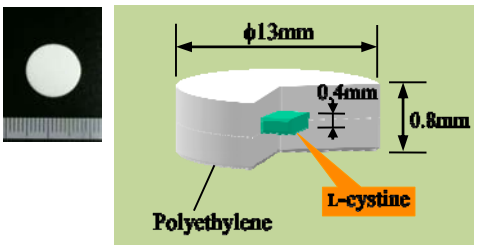

Fig. 4. Schematic illustration of the sample

The acquired time waveform is not a true waveform

of THz radiation because of the behavior of the nearly zero bias setup. The applied optical bias was as large as possible in the experiment to acquire a correct waveform. Balanced detection should be applied to EO detection to solve this problem. Although we reported balanced detection using 2D-EO sampling in Ref. [37], it has not been applied to the spectroscopic imaging using a camera yet because of the difficulty of obtaining a high SNR.

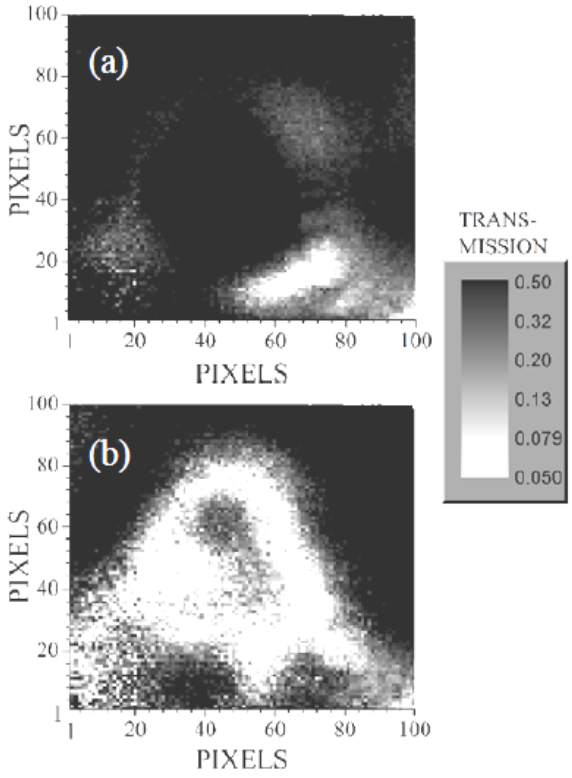

Fig. 5. Spectroscopic images at (a) 505 GHz and (b) 725 GHz. A triangular image of L-cystine is identified in a 725 GHz image

5. Conclusions

We constructed a THz spectroscopic imaging system based on 2D-EO detection. A transmissive image was observed at the fingerprint frequency of L-cystine, and the distribution of an L-cystine chip that was embedded in a pellet was successfully observed. The image size, the acquisition period, and the image quality are expected to be improved using a more efficient emitter, a high-resolution camera, and a high-stability laser source, respectively. If the image is acquired in only one frame, it is possible for spectroscopic imaging to operate at extremely high speed. When these improvements are actualized, real-time observation will become possible.

Acknowledgments

This work was supported in part by the Terahertz Optics Project for Medical Application led by Prof. J. Nishizawa, organized by the Ministry of Education, Culture, Sports, Science, and Technology of Japan.

References

[1] B. B. Hu, M. C. Nuss, Opt. Lett. **20**(16), 1716 (1995).
[2] M. C. Kemp, P. F. Taday, B. E. Cole, J. A. Cluff, A. J. Fizgerald, W. R. Tribe, Proc. SPIE **5070**, 44 (2003).
[3] N. Kanda, K. Konishi, N. Nemoto, K. Midorikawa, M. Kuwata-Gonokami, Sci. Rep. **7**, 42540 (2017).
[4] S Yamaguchi, Y. Fukushi, O. Kubota, T. Itsuji, T. Ouchi, S. Yamamoto, Sci. Rep. **6**, 30124 (2016).
[5] Z. Li, K. Meng; T. Chen, T. Chen, L. Zhu, Q.Liu, Z. Li, F. Li, S. Zhong, H. Feng, J. Zhao, Proc. SPIE **9444**, 94440P (2015).
[6] K. Meng, T. N. Chen, T. Chen, L. G. Zhu, Q. Liu, Z. Li, F. Li, S. C. Zhong, ZR. Li, H. Feng, J. H. Zhao, J. Biomed. Opt. **19**(7), 077001 (2014).
[7] S. J. Oh, S.-H. Kim, Y. B. Ji, K. Jeong, Y. Park, J. Yang, D. W. Park, S. K. Noh, S. G. Kang, Y.-M. Huh, J.-H. Son, and J.-S. Suh, Opt. Express. **5**(8), 2837 (2014).
[8] Y. B. Ji, S.-H. Kim, K. Jeong, Y. Choi, J.-H. Son, D. W. Park, S. K. Noh, T.-I. Jeon, Y.-M. Huh, S. Haam, S. K. Lee, S. J. Oh, J.-S. Suh, Opt. Express **5**(12), 4162 (2014).
[9] Q. S. Sun, Y. Z. He, K. Liu, S. T. Fan, E. P. J. Parrott, E. Pickwell-MacPherson, Quant. Imaging Med. Surg. **7**(3), 345 (2017).
[10] M. C. Nuss, J. Orenstein, Millimeter and Submillimeter Wave Spectroscopy of Solids, ed. G.. Guner, Springer, Berlin, 1998 pp.7.
[11] M. Hangyo, T. Nagashima, S. Nashima, Meas. Sci. and Tech. **13**(11)**,** 1727 (2002).
[12] Z. Jiang, X. G. Xu, X.-C. Zhang, Appl. Opt. **39**(17)**,** 2982 (2000).
[13] B. E. Cole, R. M. Woodward, D. Crawley, V. P. Wallace, D. D. Arnone, and M. Pepper, Proc. SPIE **4276**, 1 (2001).
[14] T. Yasui, E. Saneyoshi, T. Araki, Appl. Phys. Lett. **87**, 061101 (2005).
[15] D. W. van der Weide, J. Murakowski, F. Keilmann, IEEE Trans. Microwave Theory Tech. **48**(4), 740 (2000).
[16] A. M. Rollins, Jo. A. Izatt, Handbook of Optical Coherence Tomography, edited by B. E. Bouma, G. J. Tearney, Marcel Dekker, New York, 2002 Chap. 4, p. 99.
[17] M. Lai, Appl. Opt. **40**(34), 6334 (2001).
[18] W. Y. Oh, S. H. Yun, G. J. Tearney, B. E. Bouma, Opt. Lett. **30**(23), 3159 (2005).
[19] J. Xu and X.-C. Zhang, Opt. Lett. **29**(17), 2082 (2004).
[20] G. J. Kim, S. G. Jeon, J. I. Kim, Y. S. Jin, Rev. Sci. Inst. **79**(10), 106102 (2008).
[21] H. Kitahara, M. Tani, M. Hangyo, Rev. Sci. Inst. **80**(7), 076104 (2009).

[22] M. Tsubouchi, K. Nagashima, Sensors **18**(6), 1936 (2018).
[23] R. Wilk, T. Hochrein, M. Koch, M. Mei, R. Holzwarth, J. Opt. Soc. Am. B Opt. Phys. **28**(4), 592 (2011).
[24] R. J. B. Dietz, N. Vieweg, T. Puppe, A. Zach, B. Globisch, T. Gobel, P. Leisching, M. Schell, Opt. Lett. **39**(22), 6482 (2014).
[25] A. Bartels, A. Thoma, C. Janke, T. Dekorsy, A. Dreyhaupt, S. Winnerl, M. Helm, Opt. Express **14**(1), 430 (2006).
[26] C. Janke, M. Först, M. Nagel, H. Kurz, Opt. Lett. **30**(11), 1405 (2005).
[27] D. M. Mittleman, S. Hunsche, L. Boivin, M. C. Nuss, Opt. Lett. **22**(12), 904 (1997).
[28] M. C. Kemp, P. F. Taday, B. E. Cole, J. A. Cluff, A. J. Fizgerald, W. R. Tribe, Proc. SPIE **5070**, 44 (2003).
[29] Y. Hori, Y. Yasuno, S. Sakai, M. Matsumoto, T. Sugawara, V. D. Madjarova, M. Yamanari, S. Makita, T. Yasui, T. Araki, M. Itoh, T. Yatagi, Opt. Express **14**(5)**,** 1862 (2006).
[30] Z. Jiang, X.-C. Zhang, Opt. Lett. **23**(14), 1114 (1998).
[31] F. Miyamaru, T. Yonera, M. Tani, M. Hangyo, Jpn. J. Appl. Phys. **43**(4A), L489 (2004).
[32] S. R.Chinn, E. A. Swanson, J. G. Fujimoto, Opt. Lett. **22**(5), 340 (1997).
[33] H. Kitahara, M. Tani, M. Hangyo, Jpn. J. Phys. **49**(2R), 020207 (2010).
[34] M. Usami, T. Iwamoto, R. Fukasawa, M. Tani, M. Watanabe, K. Sakai, Phys. Med. Bio. **47**(21), 3749 (2002).
[35] J. Liu, L. Mao, J. Ku, B. Zha, D. Chen, W. Ding, J. Geng, Optoelectron. Adv. Mat. **11**(11-12), 677 (2017).
[36] J. Xu, Z. Lu, X.-C. Zhang, Electron. Lett. **40**(19), 1218 (2004).
[37] C. Janke, M. Forst, M. Nagel, H. Kurz, A. Bartels, Opt. Lett. **30**(11), 1405 (2005).

*Corresponding author: kitahara@fir.u-fukui.ac.jp